NONLINEAR DYNAMICS OF CRACK PROPAGATION (EXPERIMENTAL AND THEORETICAL STUDY)

O.B. Naimark, V.V.Barannikov, S.V. Uvarov

Institute of Continuous Media Mechanics, Russian Academy of Sciences,
1 Acad.Korolev street, 614013, Perm, Russia

ABSTRACT

Nonlinear dynamics of crack propagation is investigated experimentally and theoretically with a goal to clarify the nature of limiting crack velocity, the transition from steady-state to branching regimes of crack dynamics, the dynamics of crack arrest. Theoretical explanation of limiting steady-state crack velocity and the transition to branching regime was proposed due to the study of collective behavior of microcrack ensemble at the crack tip area. Experimental study of crack dynamics was carried out in the preloaded plate PMMA specimen using the high speed camera coupled with the photo-elasticity method, the point stress recording with a laser system, the failure surface roughness measurement.

Keywords: crack velocity limits, branching, crack arrest.

INTRODUCTION

The rebirth of interest in the issue of dynamic fracture is observed during last decade due to the variety of new experimental results which are not explainable within the prediction of classical fracture mechanics where it was shown [1] that the crack in infinite plane specimen has two steady-state velocities: zero and the Rayleigh speed. The recent experimental study revealed the limiting steady state crack velocity, a dynamical instability to microbranching [2,3], the formation of non-smooth fracture surface [4], and the sudden variation of fracture energy (dissipative losses) with a crack velocity [5]. This renewed interest was the motivation to study the interaction of defects at the crack tip area (process zone) with a moving crack. The still open problem in the crack evolution is the condition of crack arrest that is related to the question whether a crack velocity smoothly approaches to zero as the loads is decreased from large values to the Griffith point [6]. There is also problem at the low end of crack velocity. How a crack that is initially at rest might achieve its steady-state.

STATISTICAL PROPERTIES OF DEFECT ENSEMBLE

Microscopic and macroscopic variables for defect ensemble

Structural parameters associated with typical mesoscopic defects (microcracks, microshears) were introduced [7] as the derivative of the dislocation density tensor. These defects are described by symmetric

tensors of the form $s_{ik} = sv_i v_k$ in the case of microcracks and $s_{ik} = 1/2s(v_i l_k + l_i v_k)$ for microshears. Here $\vec{v}$ is unit vector normal to the base of a microcrack or slip plane of a microscopic shear; $\vec{l}$ is a unit vector in the direction of shear ; s is the volume of a microcrack or the shear intensity for a microscopic shear.The average of the "microscopic" tensor s_{ik} gives the macroscopic tensor of the microcrack or microshear density $p_{ik} = n\langle s_{ik} \rangle$ that coincides with the deformation caused by the defects, n is number of defects.

Statistical Model of Elastic Solid with Defects

Statistics of the microcrack (microshear) ensemble was developed in terms of the solution of the Fokker-Planck equation [7,8] in the phase space of the possible states of the microscopic variable s_{ik} concerning the size s and the orientation $\vec{v}, \vec{l}$ modes. This solution allowed the determination of the part of the free energy caused by defects.

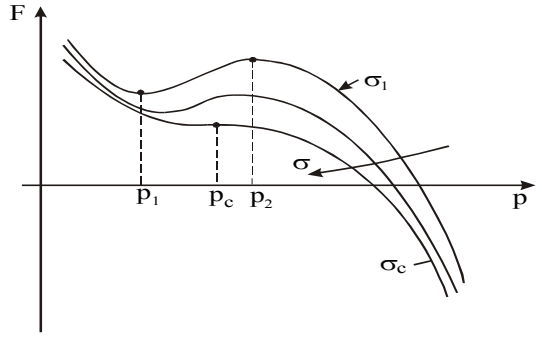

Figure 1: Free energy dependence on stress and defect density.

The free energy F for the nonlinear system "elastic solids with defects" corresponds to the form predicted by Fraenkel [9] (Fig.1). The metastability for the stress $\sigma < \sigma_c$ is the consequence of the orientation interaction in the defect ensemble. The free energy form, that was predicted by the statistical model, approaches to the Griffith form with the growth of the applied stress $\sigma \to \sigma_c$ (Fig.1). It is the consequence of the nucleation and growth of the defects with more pronounced orientation mode induced by the applied stress.

PHENOMENOLOGY OF QUASI - BRITTLE FAILURE

Free Energy

The simple phenomenological form of the part of the free energy caused by defects (for the uni-axial case $p = p_{zz}, \sigma = \sigma_{zz}, \varepsilon = \varepsilon_{zz}$) is given by sixth order expansion which is similar to the well-known Ginzburg-Landau expansion in the phase transition theory [7].

$$F = \tfrac{1}{2} Ap^2 - \tfrac{1}{4} Bp^4 - \tfrac{1}{6} Cp^6 - D\sigma\ p\ + \chi\left(\nabla_l p\ \right)^2 . \qquad (1)$$

The gradient term in (1) describes the non-local interaction in the defect ensemble in the so-called long wave approximation; A, B, C, D are positive phenomenological material parameters, χ is the non-locality coefficient.

Damage Kinetics in Quasi-Brittle Failure

The damage kinetics in quasi-brittle materials is determined by the evolution inequality [7] that leads to the kinetic equation for the defect density parameter

$$\frac{dp}{dt} = -\Gamma\left(Ap - Bp^3 - Cp^5 - D\sigma - \frac{\partial}{\partial x_l}(\chi \frac{\partial p}{\partial x_l}) \right), \qquad (2)$$

where Γ is the kinetic coefficient. Kinetic equation (2) and the equation for the total deformation $\varepsilon = \hat{C}\sigma + p$ ($\hat{C}$ is the component of the elastic compliance tensor) represent the system of constitutive equations of quasi-brittle materials with considered types of the defects.

COLLECTIVE PROPERTIES OF DEFECT ENSEMBLE

Equation (2) describes the characteristic stages of damage evolution. In the ranges of stress $\sigma < \sigma_c$ and the defect density $p < p_c$ the damage kinetics is subject to the "thermodynamic branch" corresponding to the local minimum of the free energy (Fig.1). At the approaching of stress to the critical value σ_c ($p \to p_c$) the damage kinetics is subject to specific spatial-temporal structures, which appear in the defect ensemble in the course of the interaction between defects [10,11]. These structures describe the damage localization. The subjection of damage kinetics to these structures reflects the qualitative change of the system symmetry due to the reduction of the number of independent coordinates in the damage field. The spatial-temporal structures are given by the self-similar solution of the kinetic equation (2) under the pass of the critical point p_c and reads

$$p(x,t) = \phi(t) f(\zeta), \quad \zeta = x/L_c, \quad \phi(t) = \Phi_0 (1 - \frac{t}{t_c})^{-m}, \qquad (3)$$

where $m > 0, \Phi_0 > 0$ are the parameters related to the nonlinear form of Eq.(2); L_c and t_c are the scaling parameters which can be found under the solution of the corresponding nonlinear eigen-function problem [12]. The self-similar solution (3) describes the blow-up damage kinetics for $t \to t_c$ on the set of the spatial scales $L_H = kL_c, \quad k = 1,2,...K$ [10]. The loss of metastability of the free energy under $\sigma \to \sigma_c$ (Fig.2) leads to the qualitative change of the general property of the system including the symmetry properties. In the area $\sigma > \sigma_c$ the stress field doesn't control the system behavior and the failure scenario is determined by the generation of the blow-up damage localization structures in the process zone.

ORIGIN OF CRACK TIP INSTABILITY

The kinetics of damage localization is determined by two parameters, which are given by the self-similar solution (3). These parameters are the spatial scales L_C of the blow-up damage localization and the so-called "peak time" t_c which is the time of damage localization in the self-similar blow-up regime. The velocity limit V_C of the transition from the steady-state to the irregular crack propagation is given by the ratio: $V_C \approx L_C / t_c$. The steady-state crack propagation is realized in the case when the stress rise in the process zone provides the failure time $t_f > t_c = L_C / V_C$ for the creation of the daughter crack only in the

straight crack path. The failure time t_f follows from the kinetic equation (2) and represents the sum of the induction time t_i (the time of the approaching of the defect distribution to the self-similar profile on the L_H scale) and the peak time t_c: $t_f = t_i + t_c$. For the velocity $V < V_C$ the induction time $t_i >> t_c$ and the daughter crack appears only along the initial main crack orientation. For the crack velocity $V \approx V_C$ there is a transient regime ($t_i \approx t_c$) of the creation of number of the localization scales (daughter cracks) in the main crack path. The crack velocity growth in the area $V > V_C$ leads to the sharp decrease of the induction time $t_i \to 0, t_f \to t_c$ that is accompanied by the extension of the process zone in both (tangent and longitudinal) directions where the multiple blow-up structures (daughter cracks) and, as the consequence, the main crack branching appears.

EXPERIMENTAL STUDY OF NONLINEAR CRACK DYNAMICS

Experimental setup

Direct experimental study of crack dynamics in the preloaded PMMA plane specimen was carried out with the usage of a high speed digital camera Remix REM 100-8 (time lag between pictures $10\,\mu s$) coupled with photo-elasticity method [13]. The experiment revealed that the pass of the critical velocity V_C is accompanied by the appearance of a stress wave pattern produced by the daughter crack growth in the process zone. Independent estimation of critical velocity from the direct measurement of crack tip coordinates and from pronounced stress wave Doppler pattern gives a correspondence with the Fineberg data ($V_C \approx 0.4 V_R$) [2].

Characteristic crack velocity

The dependence of crack velocity on the initial stress is represented in Fig.2. Three portions with different slopes can be shown. The existence of these portions determines three characteristic velocities: the velocity of the transition from the steady-state to the non-monotonic straight regime $V_S \approx 220\, m/s$, the transient velocity to the branching regime $V_C \approx 330\, m/s$ and the velocity $V_B \approx 600\, m/s$ when the branches behave autonomous. The characteristic velocity $V_C \approx 330\, m/s$ allowed us to estimate the peak time t_c to measure the size of the mirror zone $L_C \approx 0.3\, mm$: $t_c = L_C / V_C \approx 1 \cdot 10^{-6}\, s$.

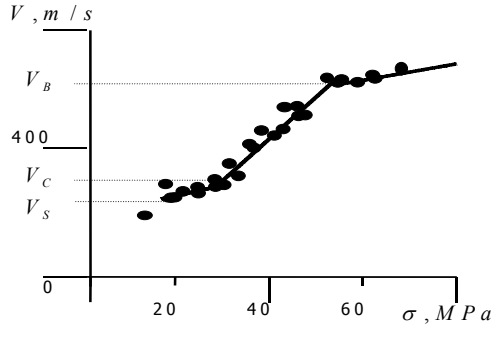

Figure 2.

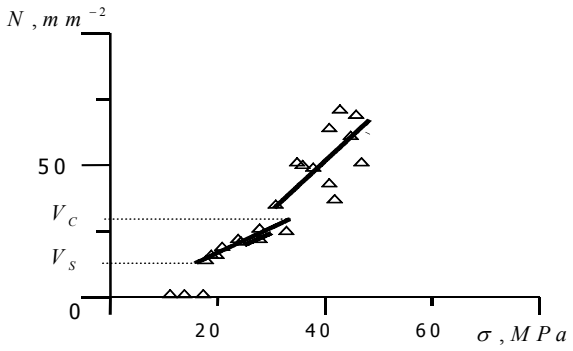

Figure 3.

In our experiments the dependence of the density of the mirror zones N on the stress also were studied (Fig.3). Actually, since the failure time for $V > V_C$ is approximately constant ($t_f \approx t_c \approx 1 \mu s$), there is a unique way to increase the crack velocity to extend the size of the process zone. The crack velocity V is

linked with the size of the process zone $L_{PZ} \sim L_H$ by the ratio $V = {L_{PZ}}/{t_c}$. Since the branch length is limited by the size of the process zone, we obtain the linear dependence of branch length on the crack velocity. This fact explains the sharp dependence (quadratic law) of the energy dissipation on the crack velocity established in [5].

Scaling properties of failure

The scaling properties of failure were studied also under the recording of the stress dynamics using the polarization scheme coupled with the laser system. The stress temporal history was measured in the marked point deviated from the main crack path on the fixed (4 mm) distance. This allowed us to investigate the correlation property of the system using the stress phase portrait $\dot{\sigma} \sim \sigma$ (Poincare cross section) for slow and fast cracks, Fig.4.

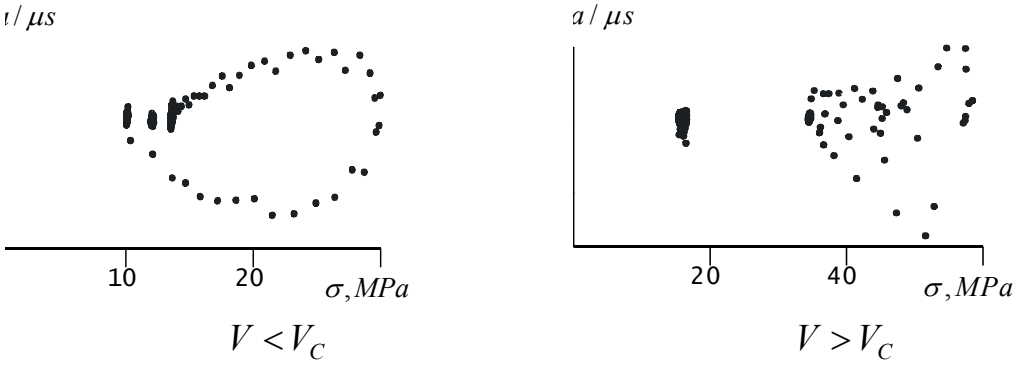

Figure 4: Poincare cross-section

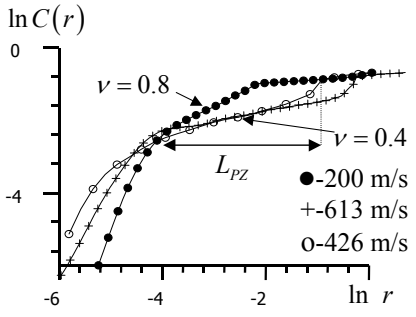

Figure 5: Correlation integral

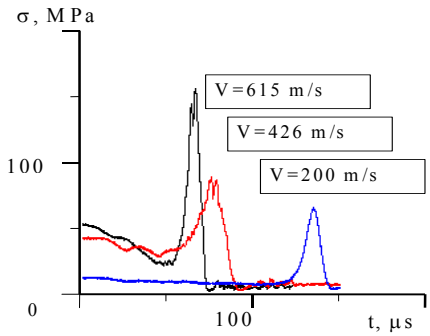

Figure 6: The stress history

These portraits display the periodic stress dynamics (Fig.4) that in the correspondence with the local ellipticity of Eq.(2) for $\sigma < \sigma_c$ ($V < V_C$) and the stochastic dynamics for $V > V_C$ corresponding to the second type of the attractor (Fig.4). The recording of the temporal stress history in the marked point for $V > V_C$ revealed the appearance of finite amplitude stress fluctuations which reflect the qualitative new changes in the process zone for the fast crack (Fig.5). The scaling properties were studied in the term of the correlation integral calculated from the stress phase pattern in the $\dot{\sigma} \sim \sigma$ space. The existence of the scales with the stable correlation index was established for the regimes $V < V_C$ and $V_B > V > V_C$. The values of the correlation indexes in these regimes show the existence of two scaling regimes with the deterministic ($V = 200 m/s$, $\nu \approx 0.8$, Fig.6) and stochastic ($V = 426, 613 m/s$, $\nu \approx 0.4$) dynamics. The extension of the portions with a constant indexes determines the scale of the process zone L_{PZ}. The length of the process zone increases with the growth of the crack velocity in the range $V_B > V > V_C$ with the maintain of the

scaling property of the dynamic system. Numerical simulation of the damage kinetics in the process zone allowed us to conclude that this scaling is the consequence of the subjection of the failure kinetics to the blow-up self-similar solution which determines the collective behavior of the defect ensemble in the process zone [14].

LOW VELOCITY LIMIT. CRACK ARREST.

In this part we have addressed the question of how a dynamic crack will approach zero velocity. This fact was discussed in [6] and it was shown considering a simplified version of the strip specimen with the radiation at the boundaries that steady-state velocity law with a square-rot behavior is expected as a function of the excess load over the Griffith load. This means that the steady-state velocity increases with an infinite slope near zero overload, but in a smooth fashion with a load. It was shown also that if the crack has no field inertia, the pass of the "trapping limit" will lead to the crack move. But if the crack has a field inertia the crack velocity will exhibit a transient oscillation. The similar conclusion can be made to compare the estimation of the crack velocity, given in [6] $V = w\sqrt{(E_e - 2\gamma)/(C(w))}$, where w is the Barenblatt cohesive zone of the crack, $(E_e - 2\gamma)$ is the Griffith static terms, $C(w)$ is material parameter, and the results predicted above statistical model. Taking in view that w is similar $L_{PZ} \sim L_H$, the root term is the inverse characteristic time t_C given by the self-similar solution. This fact allowed us to determine the range of the application of this generalized Griffith relation, where the crack can approach to the rest smoothly: $V < V_C$. For $V > V_C$, when the "wave part" of energy will increase with crack velocity, the crack arrest will appear non-smoothly for the energy metastability providing the "crack trapping". The similar view can be developed to analyze the crack overload above the Griffith value before any state motion.

This work was carried out in part during the author's stay at the LAMEFIP-ENSAM. The author is grateful to Professor J.-L.Lataillade for this opportunity and fruitful discussions.

References

1. Freund, L.B (1990) Dynamic Fracture Mechanics, Cambridge University Press, Cambridge, England.
2. Fineberg, J., Gross, S., Marder, M. and Swinney, H. (1991). *Phys.Rev.Lett*. **67**, 141
3. Sharon, E., Gross, S.P. and Fineberg, J. (1995). *Phys.Rev.Lett*., **74**, 5097.
4. Boudet, J.F., Ciliberto, S. and Steinberg, V. (1996). *J. de Physique,* **6**, 1993.
5. Sharon, E., Gross, S.P., Fineberg, F. (1996). *Phys.Rev.Lett* , **76**, 2117.
6. Holian, B.L. and Thomson, R.(1997). Phys. Rev. E, 56, 1, 1071.
7. Naimark, O.B. (1997). In: *Proceedings of the IUTAM Symposium on Nonlinear Analysis of Fracture*, Willis, J.R. (Ed). Kluwer Academic Publishers, Dordrecht, pp. 285-298.
8. Naimark, O.B. (1997). In: *Proceedings of IX Int.Conf.Fracture, B.Karihalloo* (Ed.). Sydney, Pergamon, 6, pp.2795-2806.
9. Fraenkel, Ya.I. (1952). *Journal of Technical Physics*, **22**, 11, 1857 (in Russian).
10. Naimark, O.B. (1998) . *JETP Letters*, **67**, 9, 751.
11. Naimark, O.B., Davydova, M.M. and Plekhov, O.A. (1998). In*: Proceedings of NATO Workshop "Probamat – 21 Century"*, G.Frantziskonis (Ed.). Kluwer, pp.127-142.
12. Kurdyumov, S.P. (1988). In: *Dissipative Structures and Chaos in Non-Linear Space*, Utopia, Singapure, **1**, pp.431-459.
13. Naimark, O.B. (2000). In: *Advanced in Mechanical Behavior, Plasticity and Damage*, v.1, pp.15-28, Miannay, D., Costa, P., Francois, D. and Pineau, A. (Eds). Elsevier.
14. Naimark, O.B., Davydova, M.M. and Plekhov, O.A. (2000). *Computers and Structures*, **76**, 67.